J Solution Chem (2016) 45:518–533
DOI 10.1007/s10953-016-0452-3

Complex Formation Study of Binary and Ternary Complexes Including 2,3-Dihydroxybenzoic Acid, *N*-acetylcysteine and Divalent Metal Ions

Shella Permatasari Santoso[1] · Artik Elisa Angkawijaya[1,2] · Suryadi Ismadji[3] · Aning Ayucitra[3] · Felycia Edi Soetaredjo[3] · Tran Nguyen Phuong Lan[4] · Yi-Hsu Ju[1]

Received: 22 October 2015 / Accepted: 18 January 2016 / Published online: 1 March 2016

Abstract The binary and ternary complex stability constants between 2,3-dihydroxybenzoic acid (DA) and *N*-acetylcysteine (Nac) with the divalent metal ions (M) Mn^{2+}, Co^{2+}, Ni^{2+}, Cu^{2+} and Zn^{2+} were studied in aqueous solution at 310.15 K and an ionic medium of 0.15 $mol{\cdot}dm^{-3}$ NaCl. The complexes' stability constants ($\log_{10} \beta$), refined from the potentiometric data using the Hyperquad2008 program, indicate that the ternary complexes are more stable than the binary complexes. The stability constants were supported by additional computation, refined from the spectrophotometric data using the Hypspec program. The values of the ternary complex stability relative to their binary complex ($\Delta\log_{10} K$) and the disproportionation constant ($\log_{10} X$) indicate that formation of ternary complex species $[M(DA)(Nac)]^{3-}$ is more favorable than that of species formed by two identical ligands, $[M(DA)_2]^{4-}$ or $[M(Nac)_2]^{2-}$. For the investigated M, the stability of complexes follows the trend $Cu^{2+} > Zn^{2+} > Ni^{2+} > Co^{2+} > Mn^{2+}$.

Keywords Stability constant · Potentiometry · *N*-acetylcysteine · 2,3-dihydroxybenzoic acid · Divalent metal

1 Introduction

2,3-Dihydroxybenzoic acid (DA) is a powerful iron chelator with a Fe^{3+}–DA complex stability constant ($\log_{10} K_1$) value of 20.5 [1]. The chelating ability of DA makes this compound useful in the excretion of excess iron [2]. DA naturally exists in plants such as

✉ Yi-Hsu Ju
yhju@mail.ntust.edu.tw

[1] Chemical Engineering Department, National Taiwan University of Science and Technology, Taipei 106-07, Taiwan

[2] Institute of Plant and Microbial Biology, Academia Sinica, Taipei 115-29, Taiwan

[3] Department of Chemical Engineering, Widya Mandala Surabaya Catholic University, Kalijudan 37, Surabaya 60114, Indonesia

[4] Department of Chemical Engineering, Can Tho University, 3-2 Street, Can Tho, Vietnam

Salvinia molesta, lobi–lobi fruit (*Flacourtia inermis*) and gooseberries (*Phyllanthus acidus*) [3, 4] and also in blood plasma and urine of human, as the product of aspirin metabolism [5, 6]. Biologically, DA provides health benefits due to its antioxidant, anti-inflammatory and antimicrobial actions.

DA may act as a salicylate (COO–, *ortho*-O–) type ligand or catecholate (*ortho*-O–, *meta*-O–) type ligand [7–10]. Recently, researchers demonstrated that DA also can bind metal ions such as Al^{3+}, VO^{2+}, Mn^{2+}, Cu^{2+} and Cd^{2+} as summarized in IUPAC equilibrium data report [11]. To the best of our knowledge, there are only a few reports on the stability constant of DA with divalent transition metal ions; excesses of these metal ions in human body may lead to metal toxicity. DA is often designated as a di-protic, H_2L, ligand (with 2 protonation constants, for the COO– and *meta*-O– groups) instead of tri-protic, H_3L, ligand [9–11]. Thus, in this work we attempted to treat DA as a tri-protic ligand by determining the protonation constant of the *ortho*-O– by means of spectrophotometry; this was then used for the stability constant determinations.

Ternary complex study is interesting, because it is expected that the combination of two different ligands will give synergistic effect to strengthen stability of the complex, thus dissociation of the metal complex is less likely [12]. In this study, *N*-acetylcysteine (Nac), an antioxidant that is known as glutathione precursor, mucolytic agent and neuroprotective agent, was chosen to assist the complex formation of DA [13–17]. Nac is known as a drug for treating angina pectoris, acute respiratory distress syndrome, paracetamol overdoses, ischemia–reperfusion cardiac injury, schizophrenia and bipolar disorder [18–22]. Our previous study on Nac with some divalent metal ions (Cu^{2+}, Zn^{2+}, Ni^{2+}, Co^{2+} and Mn^{2+}) indicates that the chelate complexes have stability constants in the range of 3.67 to 6.57 for $\log_{10} K_1$ and 3.69 to 6.06 for $\log_{10} K_2$, which is sufficient for the chelate complex to disassociate [23]. Thus the combination of DA and Nac was expected to give a higher stability for the complexes formed. All the complexes formed were observed in conditions comparable to human blood (i.e. 310.15 K and ionic strength of 0.15 $mol \cdot dm^{-3}$ NaCl). The equilibrium constants were refined using the Hyperquad2008 and Hypspec computer programs.

2 Chemicals and Solutions

Chemicals used in this study and their suppliers are as follows: analytical grade metal salts of nickel chloride hexahydrate ($NiCl_2 \cdot 6H_2O$, 98 %) was supplied by Alfa Aesar (Lancashire, UK); copper chloride dehydrate ($CuCl_2 \cdot 2H_2O$, 99 %), cobalt nitrate hexahydrate

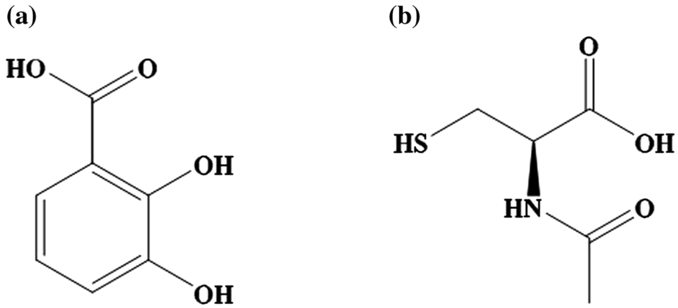

Fig. 1 Structural formulae of **a** 2,3-dihydroxybenzoic acid and **b** *N*-acetylcysteine

($Co(NO_3)_2{\cdot}6H_2O$, 98 %), and zinc nitrate hexahydrate ($Zn(NO_3)_2{\cdot}6H_2O$, 98 %) were purchased from Sigma Aldrich (St. Louis, USA); and manganese chloride tetrahydrate ($MnCl_2{\cdot}4H_2O$, 99.8 %) was supplied from Fisher Scientific (New Jersey, USA). The 2,3-dihydroxybenzoic acid (DA, $C_7H_6O_4$, 99 %) was supplied by Alfa Aesar (Lancashire, UK) and *N*-acetylcysteine (Nac, $C_5H_9NO_3S$, 99 %) was purchased from Sigma Aldrich (St. Louis, USA); their structures are shown in Fig. 1.

Sodium hydroxide (NaOH, 96 %) was provided by Yakuri Pure Chemical (Kyoto, Japan); potassium hydrogen phthalate (KHP, 99.95 %), and ethylenediaminetetraacetic acid (EDTA, $C_{10}H_{16}N_2O_8$, 98.5 %) were purchased from Sigma Aldrich (St. Louis, USA); sodium chloride (NaCl, 99.5 %) was obtained from Showa (Tokyo, Japan). Metal salt solutions were standardized by complexometry against EDTA. Carbonate free NaOH (0.1 $mol{\cdot}dm^{-3}$) used as titrant was standardized against KHP. HCl (0.03 $mol{\cdot}dm^{-3}$) was prepared and used after standardization. All solutions were prepared freshly before use, using ultra pure water obtained from an ultrapure water system with a resistance of 18.3 $M\Omega{\cdot}cm^{-1}$.

3 Experimental and Computational

3.1 Potentiometric Method

Potentiometric titrations were performed in a 150 cm^3 commercial double walled glass vessel under N_2 atmosphere. Reaction temperature was maintained at 310.15 ± 0.2 K and the ionic strength of 0.15 $mol{\cdot}dm^{-3}$ NaCl ($pK_w = -13.384$). A Metrohm 888 Titrando potentiometer, with an 805 Dosimat, Ecotrode Plus pH glass electrode and 802 rod stirrer with 804 Ti stand, was used for the measurements. The electrode used for the measurements has a precision of ±0.001 pH unit. The potentiometer, equipped with the titration software Tiamo2.3 and coupled to a personal computer, was used to control the titration and record the data. Calibration of the electrode was by means of strong acid–strong base titration, towards solution (a) defined right below, using the GLEE program [24].

For the equilibrium constant determination of binary and ternary systems, the following solutions each with a total volume of 50 cm^3 were prepared and titrated against equal increments of added 0.1 $mol{\cdot}dm^{-3}$ carbonate-free NaOH:

Table 1 Experimental condition of the investigated systems

System	Ratio	Concentration ($mol{\cdot}dm^{-3}$)		
		Metal salt	DA	Nac
Potentiometric method				
Binary	1:1	1×10^{-3}	1×10^{-3}	
	1:2	5×10^{-4}	1×10^{-3}	
	1:2.5	4×10^{-4}	1×10^{-3}	
	1:3	4×10^{-4}	1.2×10^{-3}	
Ternary	1:1:1	1×10^{-3}	1×10^{-3}	1×10^{-3}
Spectrophotometric method				
Binary	1:2	1×10^{-4}	2×10^{-4}	
Ternary	1:1:1	2×10^{-4}	2×10^{-4}	2×10^{-4}

(a) 0.003 mol·dm^{-3} HCl + 0.15 mol·dm^{-3} NaCl
(b) Solution (a) + 0.001 mol·dm^{-3} ligand DA
(c) Solution (a) + ligand DA + metal salt
(d) Solution (a) + ligand DA + ligand Nac + metal salt

The equilibrium constants include: the acid dissociation constant of ligand DA, which was determined by titrating solution (b); the metal complex stability constant, which was determined by titrating solution (c) at four different metal to DA molar ratios of 1:1, 1:2, 1:2.5 and 1:3; while ternary metal complex solution (d) was determined at a metal to DA to Nac molar ratio of 1:1:1. The total concentration of each compound used in the experiment is shown in Table 1. Each solution was thermostatted at 310.15 K and left to stand for 15 min before titration. The titration was carried out up to pH = 11.0. Each titration was repeated at least three times under controlled conditions, with a reproducibility of ±0.04 pH unit.

Computations of complex equilibrium constants were performed by processing the potentiometric data using Hyperquad2008 program [25]. The objective function was given as $U = \Sigma\ (W_i\ r_i^2)$, where W_i is the weight at the ith data point and r_i is the square of the difference between the observed and the calculated pH values. The Gauss–Newton–Marquardt method was adopted to minimize the objective function.

All constants are presented as overall formation constant in logarithm value ($\log_{10}\beta_{pqrs}$) and expressed by the following equation:

$$\mathrm{pM} + q\mathrm{Nac} + r\mathrm{DA} + s\mathrm{H} \rightleftharpoons \mathrm{M}_p\mathrm{Nac}_q\mathrm{DA}_r\mathrm{H}_s$$

$$\beta_{pqrs}\frac{\left[\mathrm{M}_p\mathrm{Nac}_q\mathrm{DA}_r\mathrm{H}_s\right]}{[\mathrm{M}]^p[\mathrm{Nac}]^q[\mathrm{DA}]^r[\mathrm{H}]^s} \tag{1}$$

The selected model was the one that gave the best statistical fit, was chemically sensible and consistent with the titration data. The species distribution of each metal complex at the observed pH was produced by the HySS2009 simulation program, based on the refined stability constants [26].

3.2 Spectrophotometric Method

Spectrophotometric measurements were conducted using a JASCO V-550 spectrophotometer in a standard 1 cm path length quartz cell. The measurement was done by scanning the spectra of the solutions of binary and ternary systems (Table 1) from 200 to 400 nm. The spectra of each solution were measured at pHs between 2.5 and 11.0, where the pH was adjusted by using 0.1 mol·dm^{-3} NaOH. The spectral data at various pHs were used to refine the formation constants using the Hypspec program [25, 27]. Spectral analyses were also carried our for the solution containing DA:Nac:metal (1:1:1) with a molar concentration of 2 × 10^{-4} mol·dm^{-3} prior to the confirmation of the ternary species formation.

4 Results and Discussion

4.1 Ligand Acid–Base Behavior

In aqueous solution, a ligand tends to deprotonate by releasing its hydrogen ion at certain pH; this deprotonation reaction property is expressed as pK_a. A higher pK_a value indicates that a more basic pH is needed to release a hydrogen ion. As a tri-protic ligand, DA possesses three functional groups, namely a carboxylic (COO–) group and two hydroxyl (O–) groups at *ortho* (*ortho*-O–) and *meta* (*meta*-O–) positions. As obtained from the potentiometry data, the deprotonation of COO– group has a pK_{a_1} value of 2.63 and the second deprotonation occurs at the *meta*-O– group with a pK_{a_2} value of 9.98. The second deprotonation is more likely to occur at *meta*-O– since this site is more reactive than the *ortho*-O–. This behavior is influenced by the electronic effect of the substituent groups and also the COO– functional group which makes the *ortho*-O– less nucleophilic than *meta*-O–. Since the *ortho*-O– is less nucleophilic, a higher basic condition was needed for its deprotonation (third deprotonation). Thus, spectrophotometry was used to determine the deprotonation of the *ortho*-O– group instead of potentiometry; the pK_{a_3} obtained for *ortho*-O– 13.00.

These pK_a values and the deprotonation order of DA are in accord with the studies of Turkel et al. [10] and Kiss et al. [28]. In the case of Nac, the first deprotonation occurs at its COO– group with a pK_{a_1} value of 3.18, followed by the thiol S– group with a pK_{a_2} value of 9.48 [23]. The pK_a values of the ligands are given in Table 2 and used for the calculation of the metal complex formation. Besides the pK_as of the ligands, the hydrolysis constants of the metal ions shown in Table 2 were also introduced into the calculation.

Table 2 Dissociation constant of DA and Nac at 310.15 K and $I = 0.15$ mol·dm^{-3} NaCl

Ligand		pK_a(SD)		
		pK_{a_1}	pK_{a_2}	pK_{a_3}
DA	This work	2.63 (4)	9.98 (2)	13.00 (2)[a]
	Ref. [10][b]	2.68	10.11	13.10
	Ref. [28][b]	2.66	9.80	>14.00
Nac	Ref. [23][c]	3.18	9.48	–
Hydrolysis constant[d]				
Cu(OH)	−7.71		Co(OH)	−9.65
$Cu_2(OH)_2$	−10.99		$Co_2(OH)$	−11.23
$Cu_3(OH)_4$	−21.62			
Zn(OH)	−8.96		Mn(OH)	−10.59
$Zn(OH)_2$	−16.90		$Mn(OH)_2$	−22.20
$Zn(OH)_3$	−28.40		$Mn_2(OH)$	−10.56
			$Mn_2(OH)_3$	−23.30
Ni(OH)	−9.86			
$Ni(OH)_2$	−19.00			
$Ni_2(OH)$	−10.70			

Standard uncertainties u are $u(T) = 0.1$ K, $u(pK_a)$ are represented by standard deviations SD in the parentheses for last place of decimal

[a] Spectrophotometry, $I = 0.15$ mol·dm^{-3} NaCl, $T = 310.15$ K

[b] Potentiometry, $I = 0.20$ mol·dm^{-3} KCl, $T = 298.15$ K

[c] Potentiometry, $I = 0.15$ mol·dm^{-3} NaCl, $T = 310.15$ K

[d] Hydrolysis constant of metal ions presented as $\log_{10}\ \beta$(SD) value, Ref. [29]

4.2 Complexation Study of Binary Systems

The divalent metal ions Cu^{2+}, Zn^{2+}, Ni^{2+}, Co^{2+} and Mn^{2+} were studied with DA and Nac. In our previous study on Nac–M chelate complexes, there were three species ([M(Nac)], $[M(HNac)]^{+}$ and $[M(Nac)_2]^{2-}$ formed in the investigated pH range (2.5–11.0). The monoprotonated $[M(HNac)]^{+}$ species, which is formed by the attachment of M^{2+} to the deprotonated COO– group, was observed in the Cu^{2+}, Ni^{2+}, Co^{2+} and Mn^{2+} systems. In this case, the proton is contributed by the H atom of the S– group. The formation of [M(Nac)] species occurs by the attachment of M^{2+} to two deprotonated groups COO– and S–. The other species was $[M(Nac)_2]^{2-}$ which is formed by the attachment of fully deprotonated Nac to the [M(Nac)] species [23].

In DA binary systems, the refinement results from Hyperquad showed that M(HDA), $[M(DA)]^{-}$, $[M(HDA)_2]^{2-}$, $[M(HDA_2)]^{3-}$ and $[M(DA)_2]^{4-}$ were the species that gave the best fit to the potentiometric data. As observed in the potentiometry titration curve in Fig. 2, the occurrence of inflection points along with pH jumps in M^{2+}–DA systems indicate the formation of metal complex species. In the case of the systems which contain ligand only, the inflection point in the titration curve indicates the deprotonation of an H atom of the ligand's donor group. An inflection point occurs when sufficient base is added to deprotonate a group (higher value of *m* indicates more base was added). In the case of

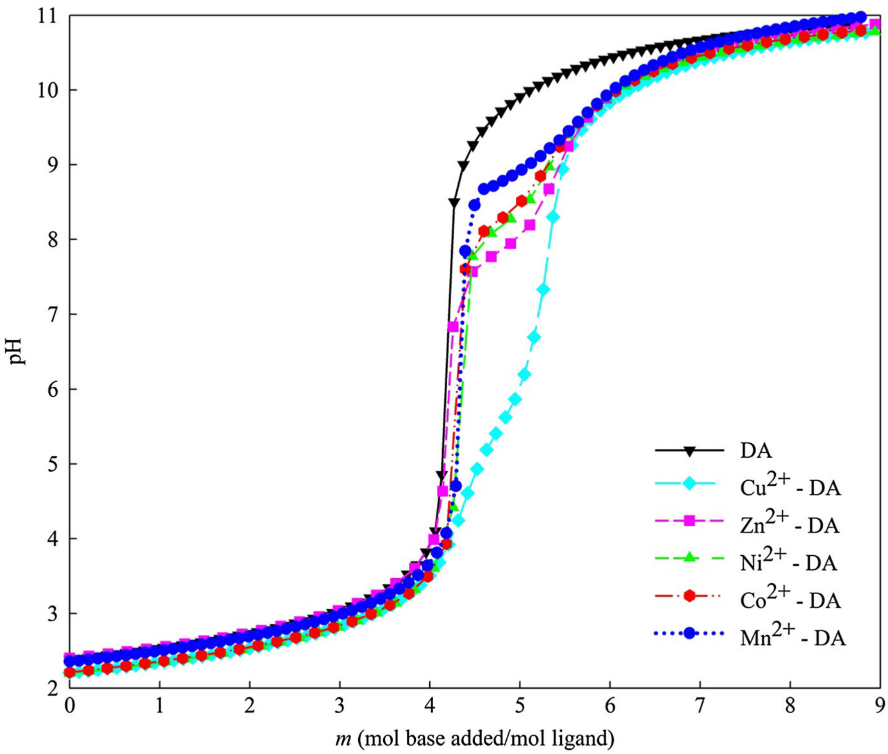

Fig. 2 Titration curve for the M^{2+}–DA system at a metal to ligand ratio of 1:2.5

DA, the inflection points occur at $m = 4.0$ and 5.0 indicating the deprotonation of COO– and *meta*-O– groups, respectively.

In the case of M^{2+}–DA, at the $m \sim 5.0$ range the M(HDA) species was formed. The inflection points concomitantly with pH jump suggest that two functional groups are involved in the formed species, namely the COO– and *ortho*-O– groups (salicylate type coordination), while the *meta*-O– group was still protonated. The deprotonation of *ortho*-O– group was promoted by the presence of metal ions that were firstly bond to the COO– group. A significant pH jump, observed from the inflection point at $m = 6.0$, suggests a stronger coordination of the metal complex compared to the salicylate type, specifically catecholate (*ortho*-O–, *meta*-O–) type, where the corresponding species in this point is $[M(DA)]^{-}$. In the studies of Kiss et al. on Cu^{2+}–DA complexes [28], Turkel et al. on Al^{3+}–DA complexes [10], and Sahoo et al. on La^{3+}–DA complexes [30], they also proposed that salicylate type complex species of DA tend to form at lower pH and catecholate type at higher pH.

At $m = 5.0$–6.0 the presence of $[M(HDA)_2]^{2-}$ and $[M(HDA_2)]^{3-}$ around this point suggests the involvement of protonated functional groups in the species. In this case, the most thermodynamically sensible forms are: two salicylate (COO–, *ortho*-O–) coordination in the formation of $[M(HDA)_2]^{2-}$, and the combination of salicylate (COO–, *ortho*-O–) and catecholate (*ortho*-O–, *meta*-O–) coordination in the formation of $[M(HDA_2)]^{3-}$, while the $[M(DA)_2]^{4-}$ species, which are formed at higher pH, suggest the coordination of two catecholates. These proposed forms with specifically mixed combination of salicylate–catecholate type and two catecholate type (at higher pH) are also in good agreement with the literature [10, 28, 30]. In addition, as observed in the titration curve, Cu^{2+}–DA exhibits the strongest pH jump indicating that Cu^{2+} possesses the strongest coordination with DA.

The overall stability constants ($\log_{10} \beta$) of M^{2+}–DA complexes are given in Table 3. There is good agreement between $\log_{10} \beta$ values from potentiometry and spectrophotometry. As summarized in Table 3, the stability of the complexes shows a decrease in the order of $Cu^{2+} > Zn^{2+} > Ni^{2+} > Co^{2+} > Mn^{2+}$ which is in accordance with the Irving–Williams order [31]. This Irving–Williams order is linear with the decrement of metal ions atomic number, where Zn^{2+} (30 pm) > Cu^{2+} (29 pm) > Ni^{2+} (28 pm) > Co^{2+} (27 pm) > Mn^{2+} (25 pm). The increase of the metal ion's electronegativity is proportional to the increase of its atomic number. In the case of Cu^{2+}, the atomic number of Cu^{2+} is smaller than Zn^{2+} but it has a more stable complex. This phenomenon is due to the smaller electronegativity of Zn (Zn (1.65) < Cu (1.99)). The high $\log_{10} \beta$ of Cu^{2+} is also due to Jahn–Teller distortion of an octahedral complex, which results in stabilization of the complex [32, 33].

The species distribution diagrams of these species were calculated from the $\log_{10} \beta$ values and graphically presented by HySS as given in Fig. 3, representatively, by Cu^{2+} and Co^{2+}. As shown in Fig. 3a for Cu^{2+} and 3b for Co^{2+}, the $[M(DA)]^{-}$ is formed at higher pH than that of M(HDA), suggesting that further deprotonation is necessary to form $[M(DA)]^{-}$, indicating the coordination of two hydroxyl group to form this species. The formation of $[M(HDA)_2]^{2-}$ and $[M(HDA_2)]^{3-}$ at lower pH compared to $[M(DA)_2]^{4-}$ species also support the assumption that the $[M(DA)_2]^{4-}$ species, which form at higher pH, are coordinated with the O– group and the other species are formed from the combination of salicylate–catecholate binding types.

In addition to metal complexes with fully deprotonated ligand $[M(DA)]^{-}$ and $[M(DA)_2]^{4-}$, the stability of adding a second ligand of the same species was calculated as the stepwise stability constant ($\log_{10} K$) value in Table 3; with $\log_{10} K_1 = \log_{10} \beta_{MDA}$ and

Table 3 Stability constants of M^{2+}–DA at 310.15 K and $I = 0.15$ mol·dm^{-3} NaCl

Species	p	q	r	s	$\log_{10}\ \beta \pm$ SD[a]		$\log_{10}\ K_{DA_1}$[b]	$\log_{10}\ K_{DA_2}$[b]
					Hyperquad[c]	Hypspec[c]		
$M = Cu^{2+}$								
M(HDA)	1	0	1	1	21.24 (1)	22.87 (3)		
$[M(DA)]^-$	1	0	1	0	15.00 (2)	14.93 (2)	15.00	
$[M(HDA_2)]^{3-}$	1	0	2	1	31.89 (2)	33.62 (4)		
$[M(DA)_2]^{4-}$	1	0	2	0	22.09 (9)	22.47 (6)		7.09
$M = Zn^{2+}$								
M(HDA)	1	0	1	1	18.30 (6)			
$[M(DA)]^-$	1	0	1	0	10.48 (4)	10.73 (2)	10.48	
$[M(HDA_2)]^{3-}$	1	0	2	1	27.26 (5)	28.81 (4)		
$[M(DA)_2]^{4-}$	1	0	2	0	16.52 (9)	16.64 (4)		6.04
$M = Ni^{2+}$								
M(HDA)	1	0	1	1	17.88 (6)			
$[M(DA)]^-$	1	0	1	0	9.67 (3)	9.76 (4)	9.67	
$[M(DA)_2]^{4-}$	1	0	2	0	15.74 (8)	16.15 (5)		6.07
$M = Co^{2+}$								
M(HDA)	1	0	1	1	17.86 (4)			
$[M(DA)]^-$	1	0	1	0	9.58 (3)	9.66 (3)	9.58	
$[M(HDA)_2]^{2-}$	1	0	2	2	35.81 (3)	35.60 (6)		
$[M(HDA_2)]^{3-}$	1	0	2	1	26.30 (4)	26.35 (5)		
$[M(DA)_2]^{4-}$	1	0	2	0	15.42 (7)	16.03 (8)		5.84
$M = Mn^{2+}$								
M(HDA)	1	0	1	1	17.26 (5)			
$[M(DA)]^-$	1	0	1	0	8.41 (3)	8.50 (3)	8.41	
$[M(HDA_2)]^{3-}$	1	0	2	1	24.81 (6)	26.61 (2)		
$[M(DA)_2]^{4-}$	1	0	2	0	14.42 (8)	14.20 (6)		6.01

Standard uncertainties u are $u(T) = 0.1$ K, $u(pK_a)$ are represented by standard deviations SD in the parentheses for the last place of the decimal

[a] p, q, r and s represent the number of metal ion, Nac, DA, and hydrogen ion, respectively

[b] $\log_{10} K$ value based on Hyperquad refinement

[c] Stability constants were refined by "Hyperquad" and "Hypspec" using potentiometric and spectrophotometric methods, respectively

$\log_{10} K_2 = \log_{10} \beta_{MDA2} - \log_{10} \beta_{MDA}$. It can be seen that $\log_{10} K_2 < \log_{10} K_1$ due to repulsion between similar ligands in one complex, which causes a decrease in stability; this is also, due to there being fewer coordination sites on the metal ion, since it has already been occupied by the first coming ligand to form the $[M(DA)]^-$ complex [34]. This suggests that the attachment of the second ligand is weaker than that of the first ligand and the formation of $[M(DA)_2]^{4-}$ species is more difficult.

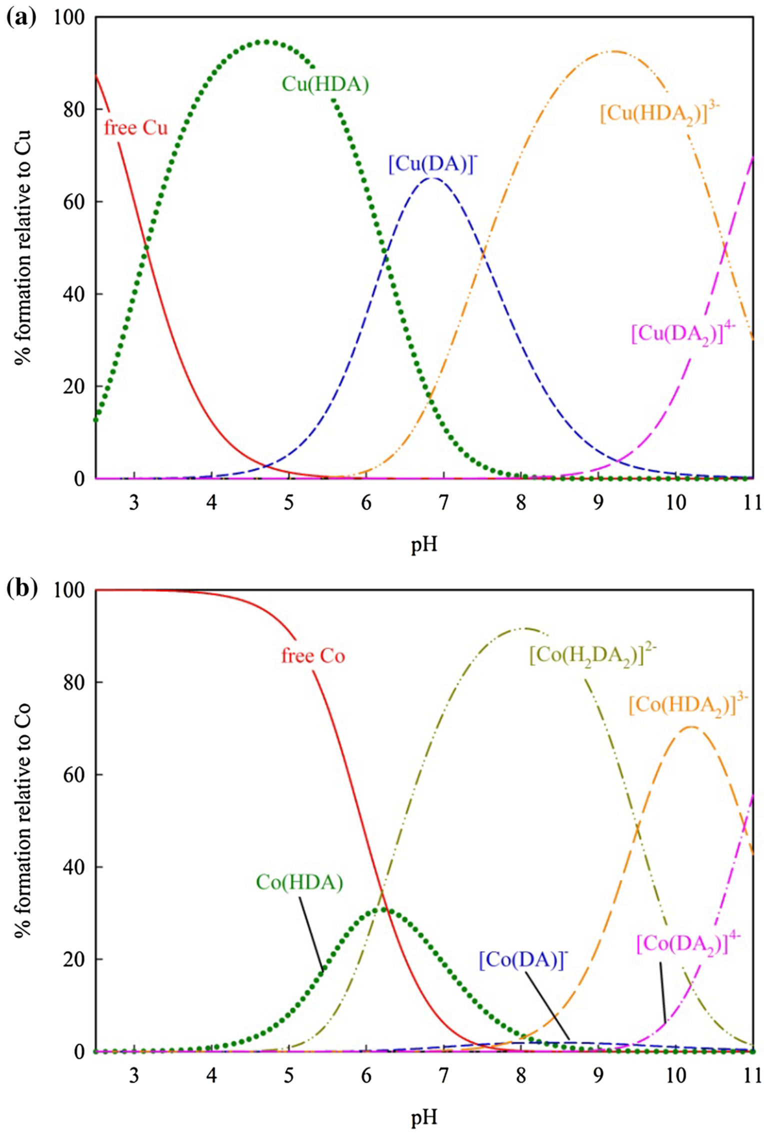

Fig. 3 Speciation diagram of binary **a** Cu^{2+}–DA and **b** Co^{2+}–DA at metal to ligand ratio of 1:2.5

4.3 Complexation Study of Ternary Systems

Formation of the ternary species $[M(HDA)(HNac)]^{-}$, $[M(HDA)(Nac)]^{2-}$ and $[M(DA)(Nac)]^{3-}$ is justified from the analysis of potentiometry data. In Fig. 4, the observed ternary titration curve exhibits greater pH jump than that of the corresponding binary system. At $m = 5.0$–6.0, a pH jump is observed suggesting a stronger coordination compared to that of the salicylate type (COO–, *ortho*-O–) coordination in binary system. Thus it can be considered that Nac coordinates through the contribution of its COO– group.

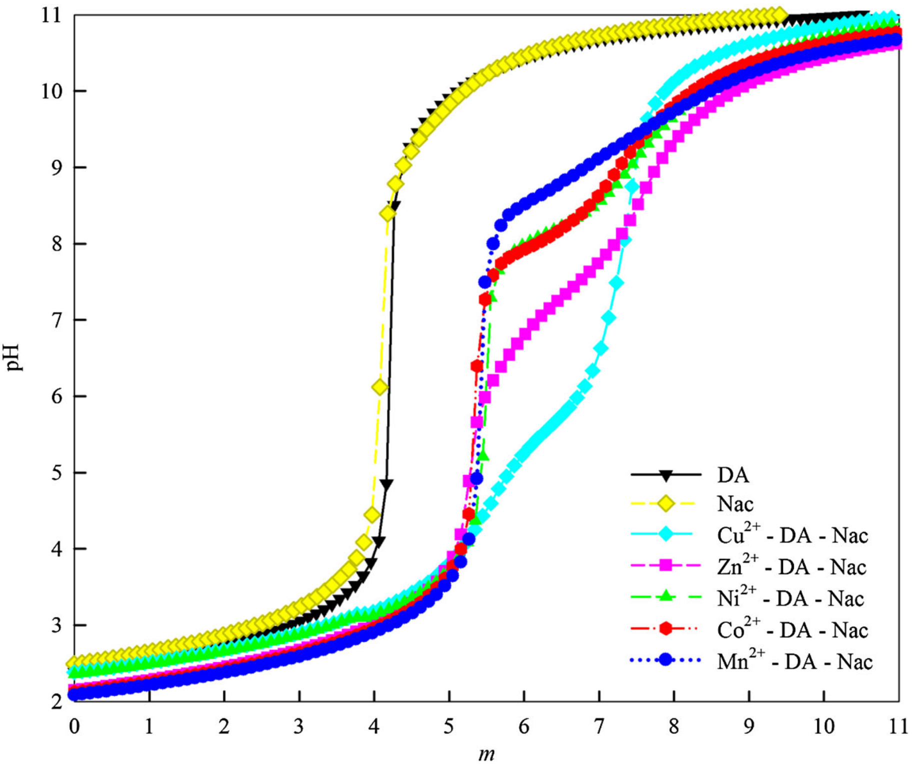

Fig. 4 Titration curve on M^{2+}–DA–Nac system at a metal to ligand ratio of 1:1:1

A significant pH jump at $m = 7.0$ suggests deprotonation, which is more likely to occur on the S– group of Nac, participated in complex formation. Further deprotonation was observed from a big pH jump at $m = 8.0$, which occurs on the *meta*-O– group of DA, suggesting the catecholate type (*ortho*-O–, *meta*-O–) coordination from DA and COO–, S– coordination from Nac.

Stability constants ($\log_{10}\ \beta$) of ternary complexes are recorded in Table 4. The results from potentiometry and spectrophotometry measurements show good agreement. The species distribution of those ternary complex species are graphically represented by Cu^{2+} and Co^{2+} complexes. As shown in Fig. 5a, the first ternary species $[Cu(HDA)(HNac)]^{-}$ was formed in the pH region where $[Cu(HNac)]^{+}$ was observed. As the $[Cu(HNac)]^{+}$ concentration decreases the formation of $[Cu(HDA)(HNac)]^{-}$ increases, suggesting that one of the two protons in the ternary species was contributed by the protonated S– group of Nac. Thus, the other proton was contributed by DA through its *meta*-O– group. Next, for $[M(HDA)(Nac)]^{2-}$ species, since the S– group of Nac is more likely to deprotonate earlier than the *meta*-O– group of DA, this suggests that the proton in the complex is contributed by the *meta*-O– group of DA. The final species $[M(DA)(Nac)]^{3-}$ was formed at highly basic pH suggesting deprotonation on the *meta*-O– group and the species was formed from the binding through catecholate type coordination of ligand DA along with (COO–, S–) coordination of Nac.

Table 4 Stability constant of ternary systems at 310.15 K and $I = 0.15$ mol·dm^{-3} NaCl

Species	*p*	*q*	*r*	*s*	$\log_{10} \beta \pm$ SD[a]		$\Delta\log_{10} K$[b]	$\log_{10} X$[b]
					Hyperquad[c]	Hypspec[c]		
$M = Cu^{2+}$								
$[M(HDA)(HNac)]^{-}$	1	1	1	2	34.77 (8)			
$[M(HDA)(Nac)]^{2-}$	1	1	1	1	28.24 (5)	29.81 (2)		
$[M(DA)(Nac)]^{3-}$	1	1	1	0	19.17 (8)	19.67 (5)	−2.47	3.55
$M = Zn^{2+}$								
$[M(HDA)(Nac)]^{2-}$	1	1	1	1	25.15 (9)	26.28 (2)		
$[M(DA)(Nac)]^{3-}$	1	1	1	0	16.38 (6)	16.66 (5)	−0.33	4.27
$M = Ni^{2+}$								
$[M(HDA)(HNac)]^{-}$	1	1	1	2	31.79 (9)			
$[M(HDA)(Nac)]^{2-}$	1	1	1	1	23.66 (7)	24.69 (3)		
$[M(DA)(Nac)]^{3-}$	1	1	1	0	14.40 (7)	14.79 (3)	−0.13	−0.09
$M = Co^{2+}$								
$[M(HDA)(Nac)]^{2-}$	1	1	1	1	23.05 (2)	23.39 (4)		
$[M(DA)(Nac)]^{3-}$	1	1	1	0	12.80 (5)	12.68 (7)	−1.06	2.27
$M = Mn^{2+}$								
$[M(HDA)(HNac)]^{-}$	1	1	1	2	30.45 (7)			
$[M(HDA)(Nac)]^{2-}$	1	1	1	1	21.59 (9)	22.15 (7)		
$[M(DA)(Nac)]^{3-}$	1	1	1	0	12.56 (4)	12.53 (3)	0.51	3.23

Standard uncertainties *u* are $u(T) = 0.1$ K, $u(\mathrm{p}K_a)$ are represented by standard deviations SD in the parentheses for the last place of the decimal

[a] *p*, *q*, *r* and *s* represent the number of metal ion, Nac, DA, and hydrogen ion, respectively

[b] $\log_{10} K$ value based on Hyperquad refinement

[c] Stability constants were refined by "Hyperquad" and "Hypspec" using potentiometric and spectrophotometric methods, respectively

The parameters $\Delta\log_{10} K$ and $\log_{10} X$ were noted as useful to indicate the behavior of ternary complexes compared to binary complexes [35–39]. $\Delta\log_{10} K$ expresses the stability of the ternary species $[M(DA)(Nac)]^{3-}$ relative to the stability of the binary species, $[M(DA)]^{-}$ and M(Nac); the value is calculated from equation:

$$\Delta \log_{10} K = \log_{10} \beta_{\mathrm{MAB}} - (\log_{10} \beta_{\mathrm{MA}} + \log_{10} \beta_{\mathrm{MB}}) \quad (2)$$

The parameter $\log_{10} X$ expresses the disproportionation tendency of binary species $[M(Nac_2)]^{2-}$ and $[M(DA_2)]^{4-}$ to form the ternary species $[M(DA)(Nac)]^{3-}$, where $\log_{10} X$ is calculated from equation:

$$\log_{10} X = 2\log_{10} \beta_{\mathrm{MAB}} - (\log_{10} \beta_{\mathrm{MA_2}} + \log_{10} \beta_{\mathrm{MB_2}}) \quad (3)$$

It was found that the complex with the highest $\log_{10} \beta$ value for its binary complex tends to have the most negative $\Delta\log_{10} K$ value, suggesting that more energy is needed to form a stable ternary complex from a stable binary complex. However, after the ternary complex is formed, it possesses a greater stability than the binary complex suggesting that the ternary complex is unlikely to disassociate back to the binary. This is supported by the

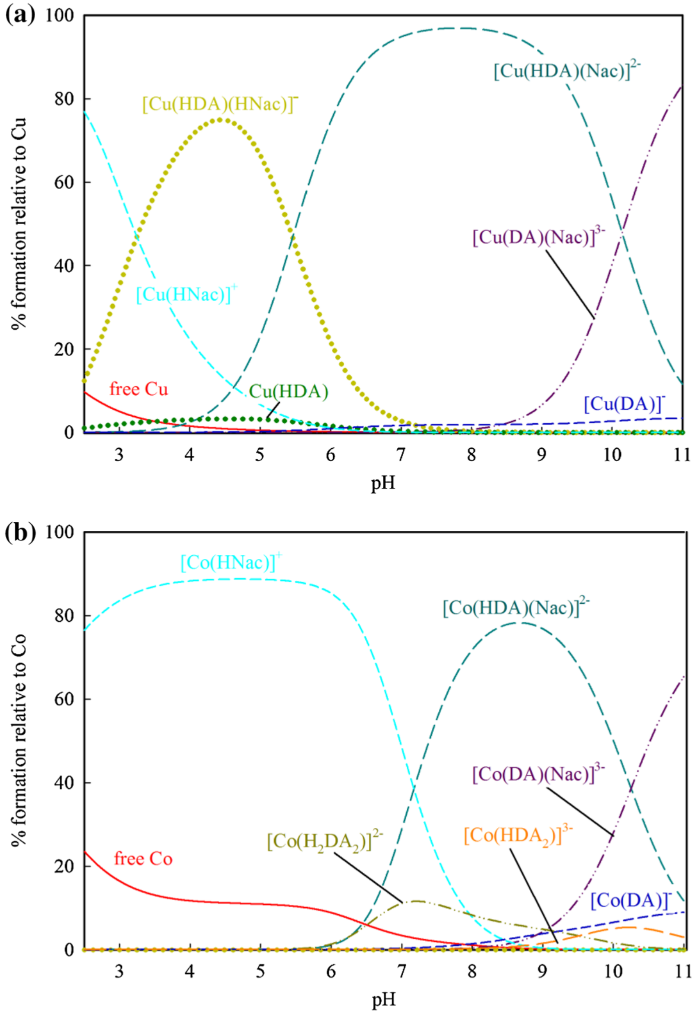

Fig. 5 Speciation diagram of ternary **a** Cu^{2+}–DA–Nac and **b** Co^{2+}–DA–Nac at metal to ligand ratio of 1:1:1

$\log_{10} X$ parameter of the ternary species, which generally have positive values, indicating that the formation of the ternary complex $[M(DA)(Nac)]^{3-}$ is more favorable than that of the binary species $[M(DA)_2]^{4-}$ or $[M(Nac)_2]^{2-}$ [40]. For instance, the $[Cu(DA)(Nac)]^{3-}$ species has the most negative $\Delta\log_{10} K$ value (−2.47) since Cu^{2+} possesses the most stable binary species $\log_{10} \beta$, indicating that less energy is gained in the formation of ternary species. However it has a positive $\log_{10} X$ value of 3.55 indicating greater stability of its ternary species. In the case of $[Mn(DA)(Nac)]^{3-}$, the $\Delta\log_{10} K$ value of 0.51 indicates that less energy is needed to form ternary species (compared to the Cu^{2+} system) and a $\log_{10} X$ of 3.23 indicates that the ternary complex of Mn is more stable than its binary species.

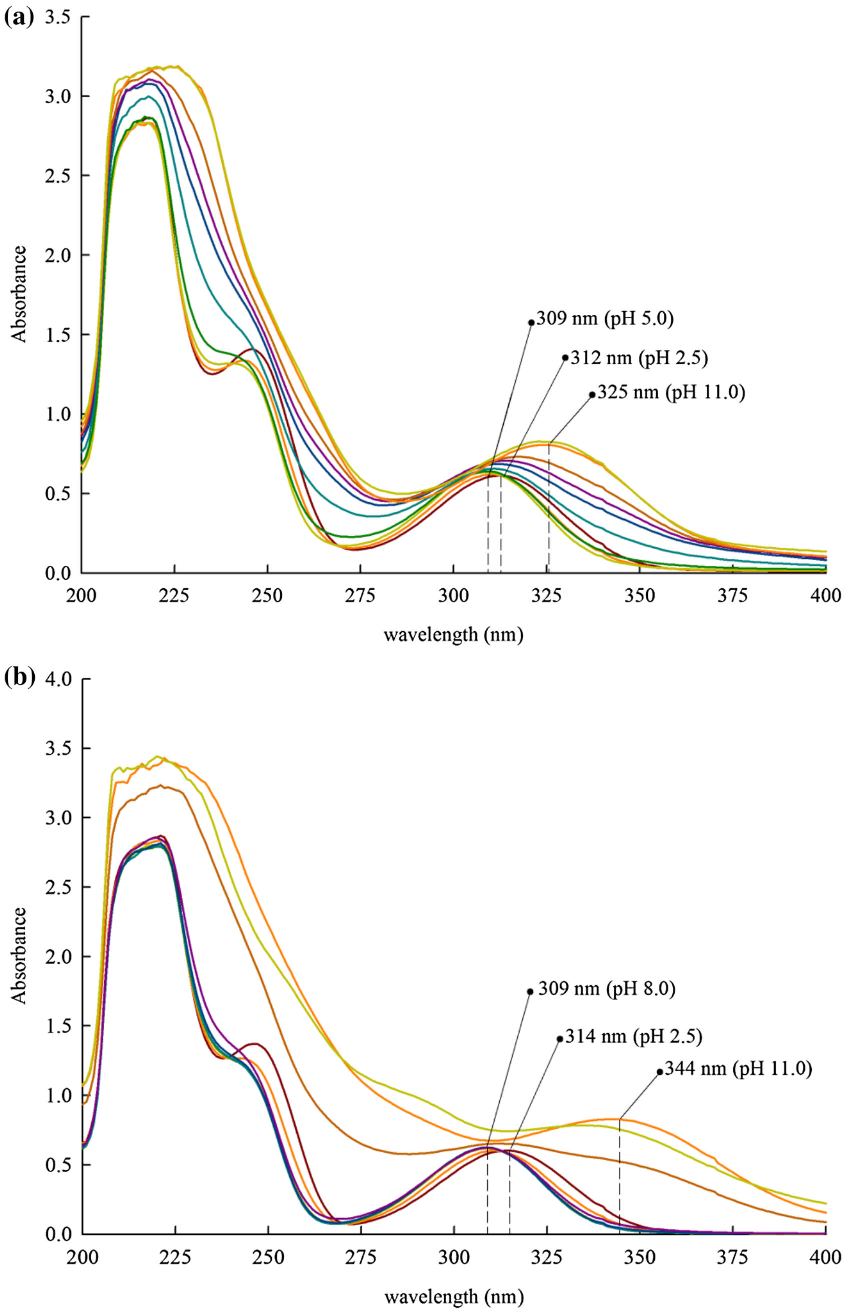

Fig. 6 Spectrum measurements of ternary **a** Cu^{2+} and **b** Co^{2+} system at M^{2+}:Nac:DA = 1:1:1

4.4 Spectrophotometric Measurements

The addition of metal ion into the ligand system yields a metal–ligand complex, which causes an alteration in the spectral behavior [37, 40]. In this work, the spectral measurements were done on ternary systems as a function of pH; as shown in Fig. 6 the wavelength range was 200–400 nm. The aromatic ring of DA gave strong absorbance at 220–250 nm for all systems. The bands observed at longer wavelength are related to the metal–ligand complex. The observed bands show similar shifts in all systems, so the Cu^{2+} and Co^{2+} systems were chosen as representative.

For the Cu^{2+} ternary system, as observed in Fig. 5a, at pH = 2.5 a band occurred at 312 nm which then exhibited a blue shift to 309 nm as the pH increased to 5.0, which was affected by the formation of $[Cu(HDA)(Nac)]^{2-}$ species. However with the pH increased to 11.0, the spectrum exhibited another red shift to 325 nm, which is more likely due to the formation of $[Cu(DA)(Nac)]^{3-}$ species. Similarly, for Co^{2+} ternary system in Fig. 5b, at pH = 2.5 a band was firstly observed at 314 nm, which then exhibited a blue shift to 309 nm as the pH increased to 8.0 but, with increase of pH to 11.0, there was a red shift to 344 nm which was caused by the $[Co(DA)(Nac)]^{3-}$ species.

5 Conclusion

Binary species of DA (M(HDA), $[M(DA)]^{-}$, $[M(HDA)_2]^{2-}$, $[M(HDA_2)]^{3-}$, $[M(DA)_2]^{4-}$) and ternary species of DA–Nac ($[M(HDA)(HNac)]^{-}$, $[M(HDA)(Nac)]^{2-}$, $[M(DA)(Nac)]^{3-}$) were found in the potentiometry analysis, supported by spectrophotometry analysis. It was found that the binding of M^{2+} to the COO– group of DA was initiated the deprotonation of the *meta*-O– group, and then formed salicylate type coordination. However, at higher pH the coordination changed to catecholate type with respect to the deprotonation of the *ortho*-O– group. While for Nac, the COO– group was also found to attach firstly to metal ions followed by the S– group as pH was increased. The stability constants of the complexes in binary and ternary system showed the same order with that of $\log_{10} \beta$ values: i.e. $Cu^{2+} > Zn^{2+} > Ni^{2+} > Co^{2+} > Mn^{2+}$. The analysis of $\Delta\log_{10} K$ and $\log_{10} X$ indicated that formation of ternary species is favorable.

Acknowledgments This work was supported by the Ministry of Science and Technology of Taiwan (NSC 102-2221-E-011-079) and National Taiwan University of Science and Technology (103M47006).

References

1. Avdeef, A., Sofen, S.R., Bregante, T.L., Raymond, K.N.: Coordination isomers of microbial iron transport compounds. 9. Stability constants for catechol models of enterobactin. J. Am. Chem. Soc. **100**, 5362–5370 (1978)
2. Graziano, J.H., Grady, R.W., Cerami, A.: The identification of 2,3-dihydroxybenzoic acid as a potentially useful iron-chelating drug. J. Pharmacol. Exp. Ther. **190**, 570–575 (1974)
3. George, S., Benny, P.J., Kuriakose, S., George, C., Gopalakrishnan, S.: Antiprotozoal activity of 2,3-dihydroxybenzoic acid isolated from the fruit extracts of *Flacourtia inermis* Robx. Asian J. Pharm. Clin. Res. **3**, 237–241 (2011)
4. Sousa, M., Ousingsawat, J., Seitz, R., Puntheeranurak, S., Regalado, A., Schmidt, A., Grego, T., Jansakul, C., Amaral, M.D., Schreiber, R., Kunzelmann, K.: An extract from the medicinal plant *Phyllanthus acidus* and its isolated compounds induce airway chloride secretion: a potential treatment for cystic fibrosis. Mol. Pharmacol. **71**, 366–376 (2006)

5. Grootveld, M., Halliwell, B.: 2,3-Dihydroxybenzoic acid is a product of human aspirin metabolism. Biochem. Pharmacol. **37**, 271–280 (1988)
6. Paterson, J.R., Blacklock, C., Campbell, G., Wiles, D., Lawrence, J.R.: The identification of salicylates as normal constituents of serum: a link between diet and health? J. Clin. Pathol. **51**, 502–505 (1998)
7. Bellaire, B.H., Elzer, P.H., Baldwin, C.L., Roop, R.M.: Production of the siderophore 2,3-dihydroxybenzoic acid is required for wild-type growth of Brucella abortus in the presence of erythritol under low-iron conditions in vitro. Infect. Immun. **71**, 2927–2832 (2003)
8. Cam, T., Irez, G., Aydin, R.: Determination of stability constants of mixed ligand complexes of the lanthanum(III) ion and identification of structures. J. Chem. Eng. Data **56**, 1813–1820 (2011)
9. Hirpaye, B.Y., Rao, G.N.: Chemical speciation of 2,3-dihydroxybenzoic acid complexes with some biologically essential metal ions in 1,2-propanediol–water mixtures. Chem. Spec. Biolavailab. **25**, 179–186 (2013)
10. Turkel, N., Berker, M., Ozer, U.: Potentiometric and spectroscopic studies on aluminium(III) complexes of some catechol derivatives. Chem. Pharm. Bull. **52**, 929–934 (2004)
11. Lajunen, L.H.J., Portanova, R., Piispanen, J., Tolazzi, M.: Stability constants for *alpha*-hydroxycarboxylic acid complexes with protons and metal ions and the accompanying enthalpy changes. Part I: Aromatic *ortho*-hydroxycarboxylic acids. Pure Appl. Chem. **69**, 329–381 (1997)
12. Lotfi, S., Mazloum-Ardakani, M., Ghasemi, J.B.: Potentiometric study of protonation and complex formation of some amino acids with Zn(II), Co(II) and Ni(II) in aqueous solution. J. Iran. Chem. Res. **2**, 247–255 (2009)
13. Brosnan, J.T., Brosnan, M.E.: The sulfur-containing amino acids: an overview. J. Nutr. **136**, 1636–1640 (2006)
14. Geier, D.A., Geier, M.R.: A clinical and laboratory evaluation of methionine cycle-transsulfuration and androgen pathway markers in children with autistic disorders. Horm. Res. **66**, 182–188 (2006)
15. Jozefczak, M., Remans, T., Vangronsveld, J., Cuypers, A.: Glutathione is a key player in metal-induced oxidative stress defenses. Int. J. Mol. Sci. **13**, 3145–3175 (2013)
16. Ozcelik, D., Uzun, H., Naziroglu, M.: *N*-Acetylcysteine attenuates copper overload-induced oxidative injury in brain of rat. Biol. Trace Elem. Res. **147**, 292–298 (2012)
17. Parcell, S.: Sulfur in human nutrition and applications in medicine. Altern. Med. Rev. **7**, 22–44 (2002)
18. Atkuri, K.R., Mantovani, J.J., Herzenberg, L.A.: *N*-Acetylcysteine—a safe antidote for cysteine/glutathione deficiency. Curr. Opin. Pharmacol. **7**, 355–359 (2007)
19. Chen, W., Ercal, N., Huynh, T., Volkov, A., Chusuei, C.C.: Characterizing *N*-acetylcysteine (NAC) and *N*-acetylcysteine amide (NACA) binding for lead poisoning treatment. J. Colloid Interface Sci. **171**, 144–149 (2012)
20. Dilger, R.N., Baker, D.H.: Oral *N*-acetyl-L-cysteine is a safe and effective precursor of cysteine. J. Anim. Sci. **85**, 1712–1718 (2007)
21. Samuni, Y., Goldstein, S., Dean, O.M., Berk, M.: The chemistry and biological activities of *N*-acetylcysteine. Biochim. Biophys. Acta **1830**, 4117–4129 (2013)
22. Zafarullah, M., Li, W.Q., Sylvester, J., Ahmad, M.: Molecular mechanisms of *N*-acetylcysteine action. Cell. Mol. Life Sci. **60**, 6–20 (2003)
23. Santoso, S.P., Chandra, I.K., Soetaredjo, F.E., Angkawijaya, A.E., Ju, Y.-H.: Equilibrium studies of complexes between *N*-acetylcysteine and divalent metal ions in aqueous solutions. J. Chem. Eng. Data **59**, 1661–1666 (2014)
24. Gans, P., O'Sullivan, B.: GLEE, a new computer program for glass electrode calibration. Talanta **51**, 33–37 (2000)
25. Gans, P., Sabatini, A., Vacca, A.: Investigation of equilibria in solution. Determination of equilibrium constants with the HYPERQUAD suite of programs. Talanta **43**, 1739–1753 (1996)
26. Alderighi, L., Gans, P., Ienco, A., Peters, D., Sabatini, A., Vacca, A.: Hyperquad simulation and speciation (HySS): a utility program for the investigation of equilibria involving soluble and partially soluble species. Coord. Chem. Rev. **184**, 311–318 (1999)
27. Gans, P., Sabatini, A., Vacca, A.: Determination of equilibrium constants from spectrophometric data obtained from solutions of known pH: the program pHab. Ann. Chim. **89**, 45–49 (1999)
28. Kiss, T., Kozlowski, H., Micera, G., Erre, L.S.: Copper(II) complexes of 2,3-dihydroxybenzoic acid. J. Coord. Chem. **20**, 49–56 (1989)
29. Pettit, L.D., Powell, K.J.: A comprehensive database of published data on equilibrium constants of metal complexes and ligands. IUPAC and Academic Software (2001)
30. Sahoo, S.K., Bera, R.K., Baral, M., Kanungo, B.K.: Spectroscopic and potentiometric study of 2,3-dihydroxybenzoic acid and its complexation with La(III) ion. Acta Chim. Slov. **55**, 243–247 (2008)
31. Irving, H., Williams, R.J.P.: The stability of transition-metal complexes. J. Chem. Soc. 3192–3210 (1953)

32. Frank, P., Benfatto, M., Szilagyi, R.K., D'Angelo, P., Longa, S.D., Hodgson, K.O.: The solution structure of $[Cu(aq)]^{2+}$ and its implications for rack-induced bonding in blue copper protein active sites. Inorg. Chem. **44**, 1922–1933 (2005)
33. Aljahdali, M., El-Sherif, A.A., Shoukry, M.M., Mohamed, S.E.: Potentiometric and thermodynamic studies of binary and ternary transition metal(II) complexes of imidazole-4-acetic acid and some bio-relevant ligands. J. Solution Chem. **42**, 1028–1050 (2013)
34. Graddon, D.P.: An Introduction to Co-ordination Chemistry, vol. 3. Pergamon Press, Canada (1968)
35. Ammar, R.A., Al-Mutiri, E.M., Abdalla, M.A.: The determination of the stability constants of mixed ligand complexes of adenine and amino acids with Ni(II) by potentiometric titration method. J. Fluid. **301**, 51–55 (2011)
36. Angkawijaya, A.E., Fazary, A.E., Ismadji, S., Ju, Y.-H.: Cu(II), Co(II), and Ni(II)–antioxidative phenolate–glycine peptide systems: an insight into its equilibrium solution study. J. Chem. Eng. Data **57**, 3443–3451 (2012)
37. Hernowo, E., Angkawijaya, A.E., Fazary, A.E., Ismadji, S., Ju, Y.H.: Complex stability and molecular structure studies of divalent metal ion with L-norleucine and vitamin B3. J. Chem. Eng. Data **56**, 4549–4555 (2011)
38. Shobana, S., Dharmaraja, J., Selvaraj, S.: Mixed ligand complexation of some transition metal ions in solution and solid state: spectral characterization, antimicrobial, antioxidant, DNA cleavage activities and molecular modeling. Spectrochim. Acta Mol. Biomol. Spectros. **107**, 117–132 (2013)
39. Sigel, A., Sigel, H., Sigel, R.K.O.: Metal Ions in Biological Systems, Biogeochemical Cycles of Elements, vol. 43. Taylor and Francis, New York (2005)
40. Chandra, I.K., Angkawijaya, A.E., Santoso, S.P., Ismadji, S., Soetaredjo, F.E., Ju, Y.-H.: Solution equilibria studies of complexes of divalent metal ions with 2-aminophenol and 3,4-dihydroxybenzoic acid. Polyhedron **88**, 29–39 (2015)